Supporting information

A nano-focused light on Stradivari violins: infrared s-SNOM reveals new clues behind craftsmanship mastery

Chiaramaria Stani,[†] Claudia Invernizzi,[‡] Giovanni Birarda,[§] Patrizia Davit,[‖] Lisa Vaccari,[*,§] Marco Malagodi,[*, ‡,⊥] Monica Gulmini[‖] and Giacomo Fiocco[‡,⊥]

[†]CERIC-ERIC, Strada Statale 14, 34149, Basovizza, Trieste, Italy

[‡]Laboratorio Arvedi di Diagnostica Non Invasiva, CISRiC, Università degli Studi di Pavia, via Bell'Aspa 3, 26100, Cremona, Italy

[§]Elettra Sincrotrone Trieste, Strada Statale 14, 34149, Basovizza, Trieste, Italy.

[‖]Dipartimento di Chimica, Università degli Studi di Torino, via P. Giuria 7, 10125, Torino, Italy

[⊥]Dipartimento di Musicologia e Beni Culturali, Università degli Studi di Pavia, Corso Garibaldi 178, 26100 Cremona, Italy

Corresponding authors: Dr. Lisa Vaccari (email: lisa.vaccari@elettra.eu) and Prof. Marco Malagodi (marco.malagodi@unipv.it)

Table of Contents

1. Description of the violins

The two well preserved violins under study were made in Cremona (Italy) by Antonio Stradivari (Cremona, 1644 − 1737) during the most important period of the historical Cremonese lutherie, the so−called "Golden Age" of the violin−maker (17th − 18th centuries). In particular, scholars are in agreement considering the decades 1690-1720 as the Stradivari's "Golden Period", during which he reached the highest technical level in his production. Instruments made during this time are usually considered of a higher quality than his earlier ones.[1]
The San Lorenzo violin was made in 1718 and bought by the court violinist of King Philip V of Spain, Mauro d'Alay. In 1757 the violin was donated to the Constantinian knights stationed in Parma at the Basilica di Santa Maria della Steccata. The journey of the violin continued from Italy to England and then to the virtuoso Giovanni Battista Viotti, before arriving, in 1823, to the Third Duke of San Lorenzo. At the beginning of the 20th century, it transitioned to the German railway engineer Georg Talbot and, since recent years, it is kept in Tokyo (Japan) as part of the Munetsugu Collection.
The Toscano violin was made in 1690, commissioned by the Marchese Ariberti, on behalf of Ferdinando de' Medici, Grand Prince of Tuscany. The violin was then sold in 1794 to an Irish collector and, at the end of 19th century, to the London Company of Hill & Sons. From 1890 to 1953, the violin was sold six times by British collectors and finally owned by the Italian State and the Accademia Nazionale di Santa Cecilia. Since 2008, the Toscano violin has been on permanent display in the Museo degli Strumenti Musicali of the Accademia Nazionale di Santa Cecilia (MUSA) in Rome.

2. Materials and Methods

- ***Violins sampling procedure and samples preparation***

A sub-millimetric sample was detached from the area under the tailpiece on the front plate of each violin (see Figure 1 in the main text) with a scalpel. In order to preserve such brittle samples and their multi-layer systems (sequence of layers, interfaces, and thickness), they were embedded into small blocks (~ 1x1x1 cm) of epoxy resin (Epofix Struers and Epofix Hardener 15:2, w:w) (Figure S1a,b). Subsequently, the sample surface of interest was exposed from the embedding resin by removing the excess of resin. Large excess of resin was removed by a sample cutting tool, then the block was dry-polished with silicon carbide fine sandpapers (up to 4000 grit for SL sample and 8000 grit for Tos), until the polished stratigraphic cross-section of the sample is exposed on one of the faces of the resin block (Figure S1c).
The polished cross-sectioned samples of San Lorenzo and Toscano violins were preliminarily observed under a visible microscope (Leica DM2700 M), as shown in Figure S1d,e. Despite the stratigraphic arrangement of the coating system of the two cross-sectioned samples was not clearly recognizable by visible light microscopy, the line highlighted by the red arrows in the panel e (Toscano violin sample) represents a deep fracture separating the coating system from the first line of the wood cells and demonstrates the fragility and brittleness of this sample. A comparable fracture has been observed also in the San Lorenzo violin sample, despite less visible by optical microscopy.
In order to highlight the organization of the coating system, an Olympus BX51TF microscope equipped with an Olympus U-RFL-T for UV light (350.7 nm) was used. As a matter of fact, due to the specific native fluorescence properties of the diverse materials composing the coating system, UV light enhances sample features and characteristics providing a more detailed overview of the stratigraphies of the cross−sectioned samples (See Figure S2).[2] This approach is a routine in the examination of this type of samples.

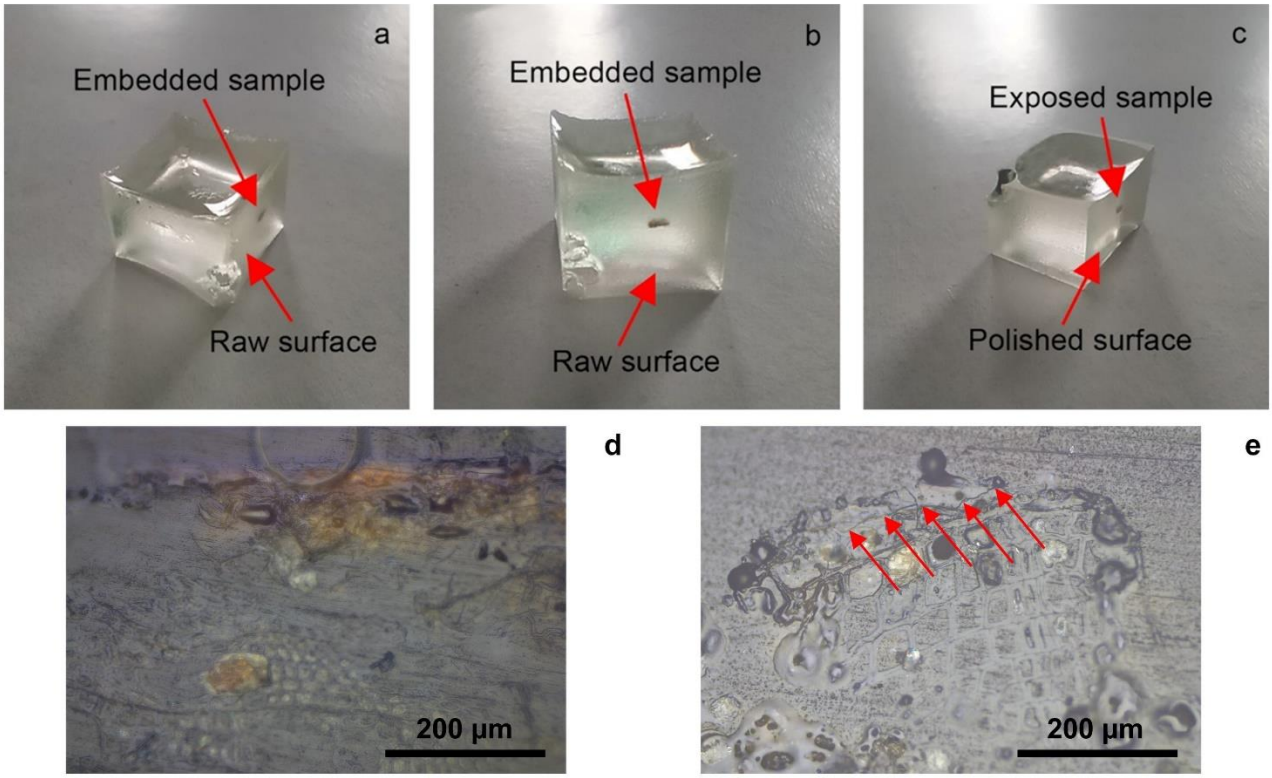

Figure S1. Images of the epoxy resin block with the embedded micro-sample: a,b) the micro-sample is completely embedded in the epoxy resin; c) the surface is polished and the stratigraphy is exposed; d,e) Optical images (20x magnification) of the polished cross-sections of San Lorenzo and Toscano violin, respectively. Red arrows point a fracture separating the coating system from the first line of the wood cells.

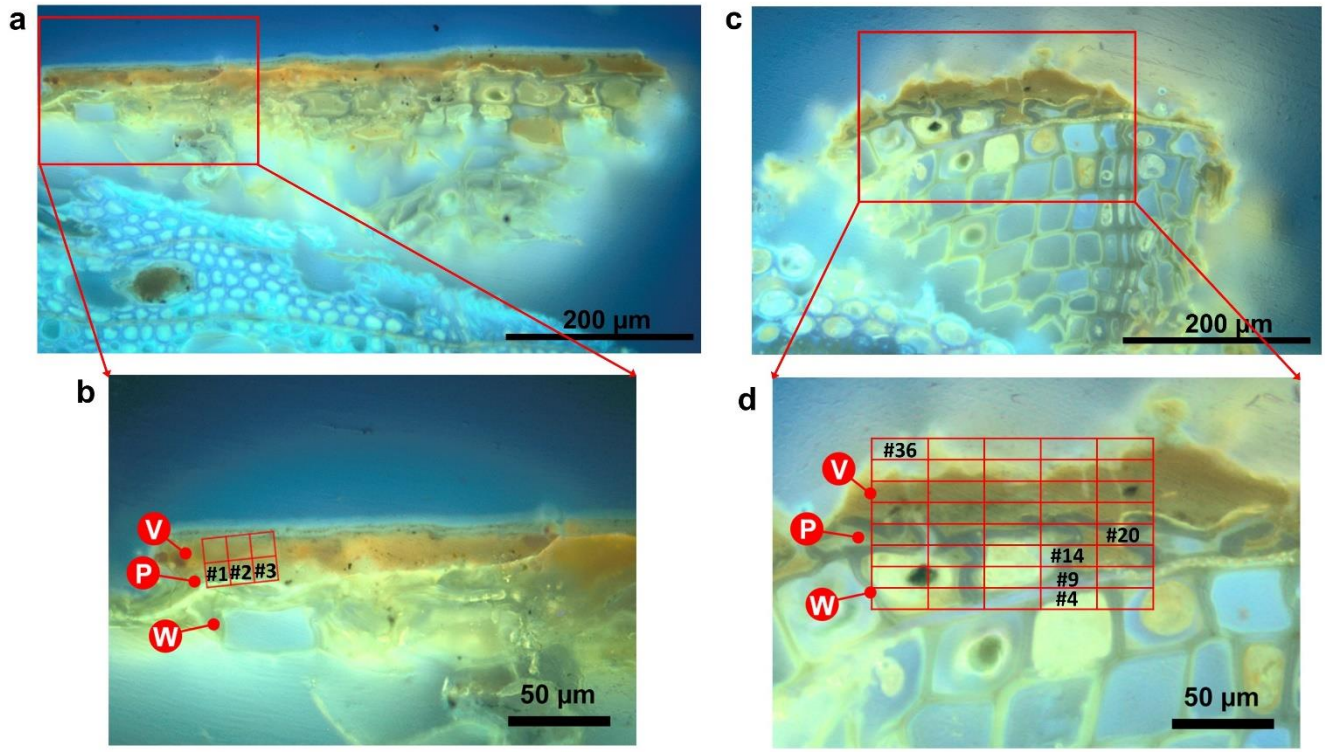

Figure S2: UV-autofluorescence images of the two cross-sectioned samples: a,b) San Lorenzo (20x and 50x magnification, respectively), c,d) Toscano violin (20x and 50x, magnification respectively). The layers identified under the UV-microscope and described in the main text are indicated by capital letters: V= Varnish, P= Preparation layer, W= Wood. The red grids in panels b and d highlight the areas mapped with SR FTIR-microscopy in reflection mode. Grid tails are overlaid on the UV-

autofluorescence images according with the lateral resolution set by closing the knife-edge apertures of the Hyperion 3000 Vis-IR microscope (San Lorenzo 15×15 μm^2; Toscano 30×10 μm^2).

- ***Preparation of the collagen reference sample***

Collagen from rat tail tendon, purchased from Sigma Aldrich, was prepared as a 0.5 $\mu g \cdot L^{-1}$ solution in 0.2 $mol \cdot L^{-1}$ acetic acid. 5 µl of the solution were spotted on a 1x1 cm^2 (100) double polished low-doped silicon substrate covered by 50 nm of evaporated gold. The sample was then let dry in air for few minutes before measurements.

- ***SR micro-FTIR data acquisition and analysis***

SR-FTIR microscopy measurements were performed at the Chemical and Life Sciences branch of Infrared beamline at Elettra Sincrotrone Trieste, SISSI-Bio.[3] Measurements were performed in reflection geometry using the in-vacuum interferometer Vertex 70v coupled with the Vis-IR Hyperion 3000 microscope (Bruker Optics GmbH) equipped with single point mercury-cadmium-telluride detector (MCT-A, Infrared Associates Inc., Stuart, Florida) and a Cassegrain objective (20x, NA=0.6). The chemical maps were collected setting the lateral resolution according with the samples' stratigraphy, closing knife-edge apertures at 15×15 μm^2 and 30×10 μm^2 for the San Lorenzo and the Toscano respectively. Spectra were collected in the 4000−750 cm^{-1} spectral range at 4 cm^{-1} spectral resolution, averaging 512 scans at 120 KHz scanner speed. Reference spectra were collected every five spectral point on a clean reflective gold surface with the same experimental parameters.
Collected spectra were subject to smoothing (Savitzky−Golay method, 15 wavelengths gap size and 2nd polynomial order) and then Kramers−Kronig transformed (range 4000-750 cm^{-1}, resulted spectra in absorbance) using the dedicated routines of OPUS 7.5 software (Bruker Optics Billerica, MA, US).
Univariate chemical maps presented in Figure 2 were generated with OPUS 7.5 software, by integrating the spectral range 1700-1590 cm^{-1}, and plotting in 2D the distribution on the integral intensities exploiting a chromatic scale ranging from red (highest values) to blue (lowest values). The 2D-countinous plot visualization was chosen. The spectral profiles shown in Figure 2c,d have been generated by cutting the spectral range 1750−1525 cm^{-1} and applying a 16-points rubberband baseline. The spectra have been plotted by OriginPro 9.7 (OriginLab Corporation, Northampton, MA, USA).
Since a possible interference of the epoxy resin, employed for sample preparation, on amide I and amide II bands in the 1750−1525 cm^{-1} spectral range cannot be excluded a priori, it was evaluated as follows. Figure S3a shows the micro-FTIR spectrum collected at location #36 of the Toscano mapped region, also highlighted in Figure S2d, in the 1800-1400 cm^{-1} spectral region, that clearly identifies the epoxy resin. The spectrum is mainly characterized by an intense peak, in the considered spectral region, centered at 1510 cm^{-1} and assigned to the ν C−C of aromatics rings.[4] The 2D false color map obtained integrating the spectral range 1525−1490 cm^{-1} is shown in Figure S3b and highlights that the resin is manly localized in the upper part of the measured area for the Toscano violin, and basically follows the rim of the embedded sample (see also UV-autofluorescence image in Figure S2d). In the spectral region of amide I and II bands, the epoxy resin has a further absorption peak at around 1610 cm^{-1}, much less intense with respect to the one centered at 1510 cm^{-1}. The false color map obtained by integrating the 1625−1590 cm^{-1} spectral region, shown in Figure S3c, substantially overlays with the IR map in Figure S3b, while it does not with the false color map obtained by integrating the amide I spectral region (1700−1590 cm^{-1}), shown in Figure S3d. In Figure S3e, the spectral profiles of the mapped points #4, #9, #14 and #20 at the wood-ground interface, taken into consideration for the present study to investigate the possible application by Antonio Stradivari of a protein-based ground coat, are compared with the spectrum of the epoxy resin at point #36. Despite the spectra shown in Figure S3e may reveal the presence of the absorption peak at 1510 cm^{-1}, it must be considered that the band ratio 1510:1610 cm^{-1} is around 1:4, therefore it is reasonable to assume that the spectral interference of the peak at 1610 cm^{-1} of epoxy resin on amide I band is negligible with respect to the proper protein contributions or contributions from other molecules. For the San Lorenzo sample, the mapped region did not include pure resin points, but the same conclusions can be drawn, as shown in Figure S4. The same conclusions apply also for the data from the points selected for nano-FTIR analysis, where the peak at 1510 cm^{-1} was not even detectable (see Figure 3 in the main text).

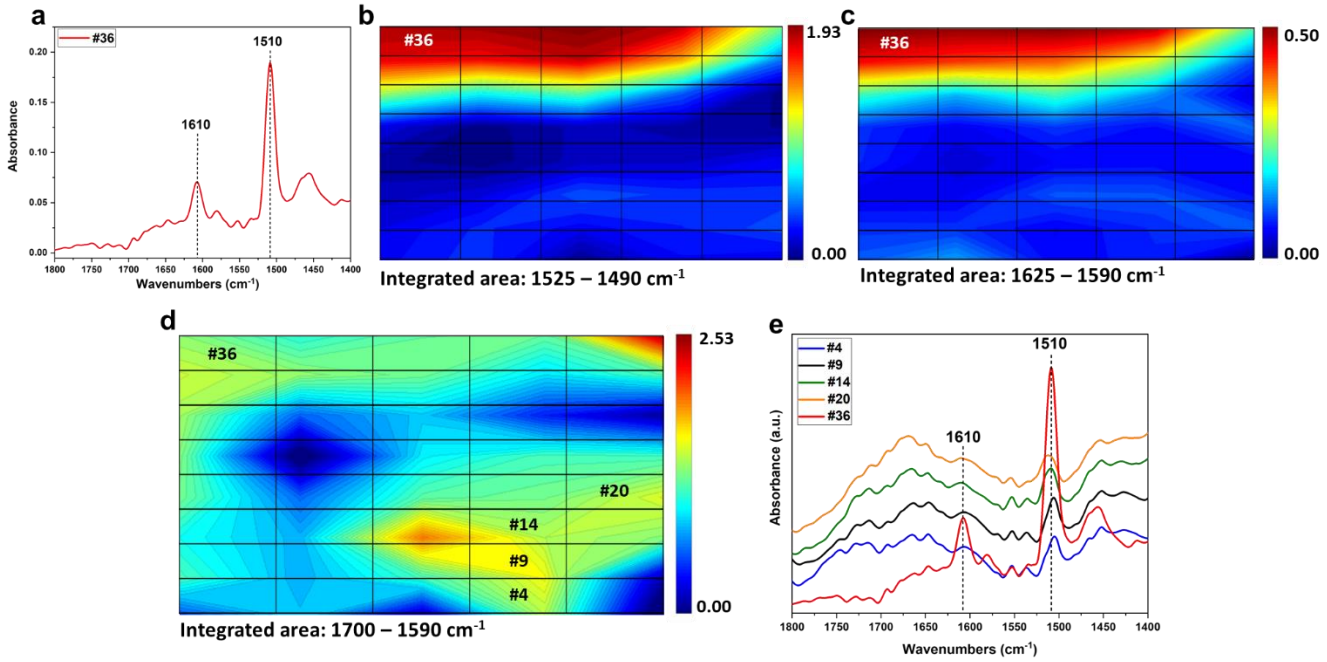

Figure S3: a) SR-FTIR spectrum extracted from point #36 of Toscano violin. b-d) False-colour maps obtained integrating the spectral ranges 1525-1490 cm^{-1} (panel b), 1625-1590 cm^{-1} (panel c) and 1700-1590 cm^{-1} (panel d). e) SR-FTIR spectra of the selected points as marked in panel d.

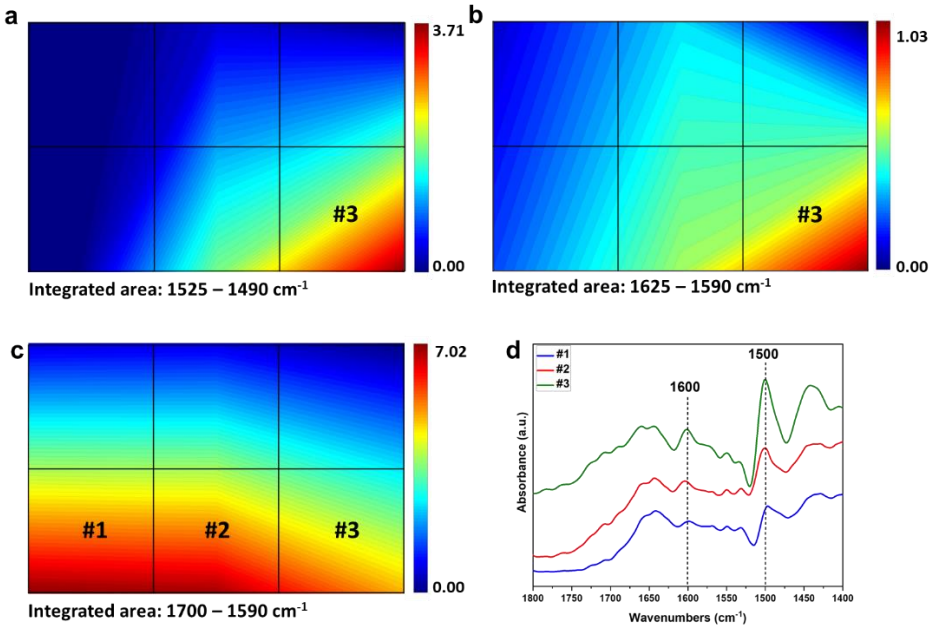

Figure S4: a-c) False-colour maps obtained integrating the spectral ranges 1525-1490 cm^{-1} (panel a), 1625-1590 cm^{-1} (panel b) and 1700-1590 cm^{-1} (panel c). d) SR-FTIR spectra of the selected points as marked in panel c.

- ***IR s-SNOM data acquisition and analysis***

Infrared s-SNOM measurements were performed at SISSI-Bio (SISSI-nano end station)[3] by means of a NeaSNOM microscope (Attocube GmbH, Munich-Harr, Germany) coupled with a fiber-based broadband mid-IR laser source using a difference frequency generator (DFG), (Toptica Photonics AG, Gräfelfing, Germany), covering the range 650-2300 cm^{-1}. The data were collected setting the operating interval between 1200-1800 cm^{-1}, with an average power of 800 μW. Metallic tips (ARROW-NCPt from NanoWorld, Matterhorn, Switzerland) with a cantilever resonance frequency of 260 kHz, and a tip radius of about 20 nm were used. The AFM image size was adjusted according to the sample stratigraphy, keeping a constant pixel size of 100 nm. Two areas of 30×10 μm^2 and 20×20 μm^2 were scanned for the San Lorenzo violin, and two areas of 20×20 μm^2 and 15×20 μm^2 for the Toscano violin. Within these regions, around ten FTIR spectra have been collected using an MCT detector (Infrared Associates Inc., Stuart, Florida), averaging 16 scans at a spectral resolution of 8 cm^{-1}, setting the zero-filling factor at 4. Each spectrum is the second order amplitude ($s(\omega)$) and phase ($\phi(\omega)$) of the backscattered light as a function of frequency, ω. For the two violin's samples, the reference spectra were measured on a clean piece of silicon wafer placed near to each

cross-section. AFM and IR data were acquired in tapping mode, setting the tapping amplitude at around 120 nm (with the approach at 80% of the free tapping amplitude).
The same measurement parameters were used for recording the collagen type I spectra, with the only difference that the reference spectra were directly collected on a clean region of the golden-coated silicon wafer where the standard collagen was spotted.
Spectra were analyzed with the neaPLOT™ software package (Ver. 1.8.270, Attocube GmbH, Munich-Haar, Germany). All the spectra were 8 points smoothed using moving average algorithm, cut in the 1770- 1310 cm^{-1} spectral range, corrected for phase and offset. Background correction, morphological profiles and roughness calculation on AFM images were done by Gwyddion 2.55.[5] The profiles calculation has been performed applying the "Profile" tool by drawing 2 to 4 profile lines (thickness 35 pixels) for each measured area. The roughness calculation was performed by the "One-Dimensional Roughness Parameters", averaging on the entire AFM image areas and setting the cut-off parameter at 1.5 µm for both the San Lorenzo and Toscano samples. All the spectra were plotted with OriginPro 9.7 (OriginLab Corporation, Northampton, MA, USA).

3. AFM analysis of the sample surface

Details on the sample surface morphology were obtained by inspecting the AFM images that correlate IR s-SNOM measurements. The AFM height images were exported and analyzed with Gwyddion 2.55 software. The measured areas on both the San Lorenzo and the Toscano samples show wavy surfaces characterized by scratches (blue regions in Figure S5 a,c and S5 e,h). The average width of them ranges approximatively between 6 to 11 µm and they are about 300 to 500 nm deep (see Figure S5 b,d and f,i). Such scratches could have originated during the first steps of the cross-section polishing by papers with particle size around 9 µm (i.e 4000 grits), that is almost in the same range of the scratch width. Moreover, for the Toscano, an almost homogeneous pattern of parallel scratches (Figure S5 g,j), around 0.5 − 1 µm wide and 10 to 20 nm deep, was observed and possibly reflects the finer grits (8000 grit with particle size of 1 − 3 µm) of the micro-mesh abrasive powder used for the polishing. The morphology of the cross-section surfaces is not surprising, since these samples were manually prepared, often by different operators, and therefore a perfect reproducibility cannot be expected. Nevertheless, it is indicative of the details that could become relevant when a nanoscale approach is employed on polished cross-sections prepared for a micro-scale analysis. For such samples, a single-point nano-spectroscopic approach may be much more useful and informative with respect to image larger areas, letting to optimize the instrument according with the sample micrometric surface wave-like modulation.
Going down to the nanoscale, the roughness was calculated by the "One-Dimensional Roughness Parameters" tool of Gwyddion 2.55 software, particularly useful in case of "wave-like" surface profiles. The calculation gave comparable roughness values for the two samples, in the range of 3 nm, below the radius of curvature of the AFM-tip used for scanning the samples.

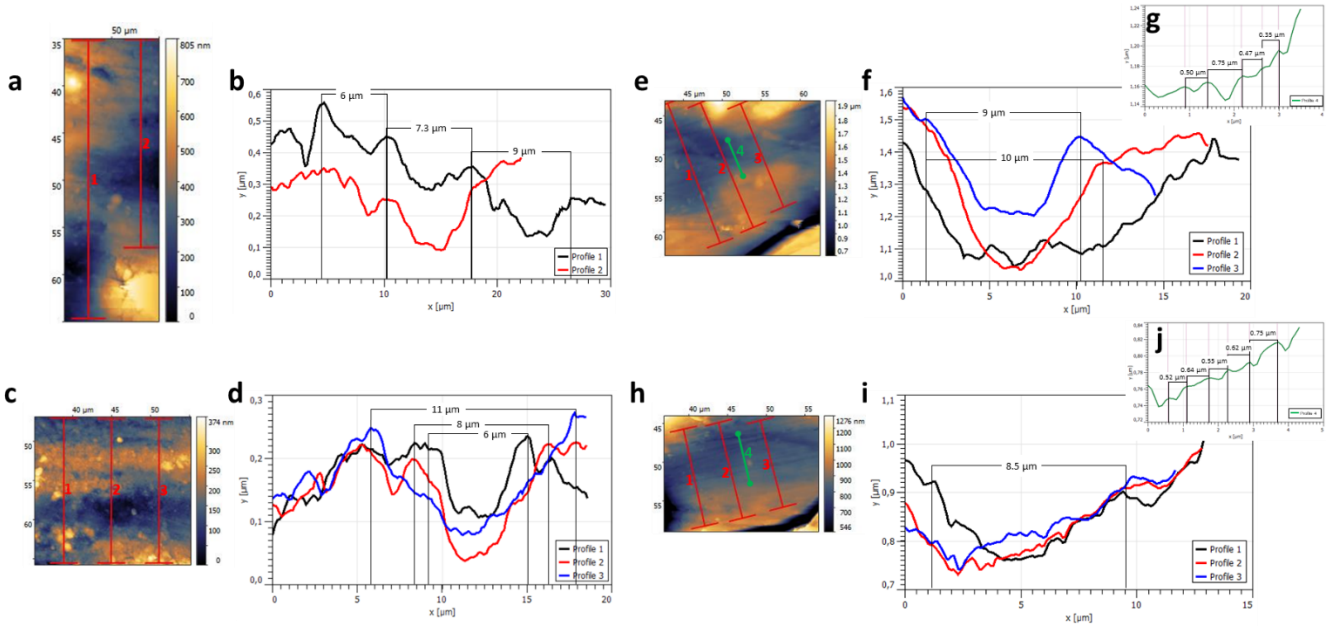

Figure S5: Profile analysis: a,b) SL-A area and associated profiles along 1 and 2 lines. c,d) SL-B area and associated profiles along 1, 2 and 3 lines. e-g) Tos-A area, associated profiles along lines 1, 2 and 3 and line 4 (profile in the g inset). h-j). Tos-B area, associated profiles along lines 1, 2 and 3 and line 4 (profile in the j inset).

References

(1) Cacciatori, F. Liuteria Cremonese: Un'antica Tradizione. In *Lo scrigno dei tesori, Fondazione Museo del Violino Antonio Stradivari Cremona*; Cacciatori F. (ed.), Ed.; 2014; pp 16–19.

(2) Sandu, I.; Joosten, I.; Leal, N. Optical Imaging Applications for the Study of Cultural Heritage Artifacts. In *Advances in Laser and Optics Research - Volume 11*; Artkin, W. T., Ed.; Nova Science Publishers: New York, 2015.

(3) Birarda, G.; Bedolla, D.; Piccirilli, F.; Stani, C.; Vondracek, H.; Vaccari, L. Chemical Analyses at Micro and Nano Scale at SISSI-Bio Beamline at Elettra-Sincrotrone Trieste. In *Biomedical Vibrational Spectroscopy 2022: Advances in Research and Industry*; Huang, Z., Ed.; SPIE, 2022; p 31. https://doi.org/10.1117/12.2607751.

(4) Socrates, G. *Infrared and Raman Characteristic Group Frequencies. Tables and Charts*; 2001. https://doi.org/10.1002/jrs.1238.

(5) Nečas, D.; Klapetek, P. Gwyddion: An Open-Source Software for SPM Data Analysis. *Open Phys.* **2012**, *10* (1). https://doi.org/10.2478/s11534-011-0096-2.